Archaeometric study of mortars from the Pisa's Cathedral Square (Italy)

Marco Lezzerini[a,*], Simona Raneri[a], Stefano Pagnotta[a], Stefano Columbu[b], Gianni Gallello[c]

[a] Department of Earth Sciences, University of Pisa, Via S. Maria, 53, 56126 Pisa, Italy
[b] Department of Chemical and Geological Sciences, University of Cagliari, Via Trentino, 51, 09127 Cagliari, Italy
[c] Department of Archaeology, University of York, King's Manor, YO17EP York, UK

ABSTRACT

The present work is focused on the study of forty-two mortars used in the construction of both Roman buildings, old Pisa's Cathedral and Modern structures in the Miracles Square (Italy). This area, included since 1987 in the World Heritage List of the UNESCO, is famous for the presence of an important historical complex built in the Middle Ages (the Cathedral, the Baptistery, the Leaning Tower and the Monumental Cemetery). The archaeologists discovered some structures related to more ancient periods: the Roman *domus* (1st–5th centuries) and the older cathedral with its foundations and crypt (10th century). Based on OM, XRF, XRPD, TG-DSC and SEM-EDS analyses, the main characteristics of binder and aggregate of the mortars have been determined, and some raw materials used for the production of the analysed binding materials have been identified.

1. Introduction

The study of ancient mortars has an important role in the knowledge of complex archeological sites, providing essential information about building technologies used in the past [1–5], construction phases [6–9] building materials features [10–12] provenance issues [13–15], evaluation of binder/aggregate ratio [16] as well composition for restoration aims [17–19]. The use of mortars in architecture was carried out since prehistoric time until the present days [20–24]. Lime mortars had a very important key function in Roman architecture; in fact, Romans used mortars to make the load-bearing walls and partition walls of rooms, to plaster them for protection purpose or to decorate their surface with paintings [25,26]. Usually, they used both quick lime and hydraulic binders, obtained by adding pozzolanic materials characterized by hydraulic properties, the latter to increase strength of mortars [27–29].

Mortars characterization is usually performed by combining macroscopic observations, minero-petrographic [30,31] and micro-chemical techniques [32–34]. The preliminary naked-eye analysis of samples, followed by thin section studies, is useful for acquiring basic information on the main characteristics and properties of these artificial materials. Data obtained by X-ray fluorescence, X-ray powder diffraction (XRPD), scanning electron microscopy with energy-dispersive X-ray spectroscopy (SEM-EDS) [35–39] and thermogravimetric analysis (TGA) [40,41] complement a lot the information obtained by preliminary studies, allowing to obtain a full characterization of both binder and aggregate fractions. In the framework of chemical techniques, Rare Earth Elements (REE) measured by ICP-MS [6] and Micro-Laser-Induced Breakdown Spectroscopy (μ-LIBS) analysis [42] have been successfully applied for identifying construction phases and for obtaining elemental mapping without sample preparation, respectively.

With these drawbacks, a multi-methodological approach, including classical minero-petrographic techniques and advanced chemical analysis, has been applied to characterize Roman and Medieval mortars from the Roman *domus* (1st–5th centuries) and the old Pisa's Cathedral (dated to the 10th century) [43] (Fig. 1). The structures were discovered during the archaeological excavations carried out in 2003–2009 in Miracles Square (Pisa, Italy), the latter included since 1987 in the World Heritage List of the UNESCO, being characterized by one of the most important historical complex of the Middle Age, whose construction started at the second half of the 11th century. The *domus* was characterized by walls made up of blocks of calcarenite (*Panchina Livornese*) and marble from *Monte Pisano* [44,45] jointed by mortars, and by decorations consisting in marbles, mosaics and painted plasters. These *domus* were abandoned during the Late Antiquity (5th–6th centuries); in the Early Middle Age (6th–7thcenturies) the area had a central role in the religious life of Pisa, as testified also by the old Baptistery, discovered in the first half of the 20th century under the structures of the *Monumental Cemetery*. About the old Cathedral, which foundations passed away the north-west side of the actual cathedral, it was characterized by three naves and an apse with a crypt, built by averagely small stones mainly consisting in reused materials (such as limestones and marble from *Monte Pisano*, *Panchina* calcarenite, violet
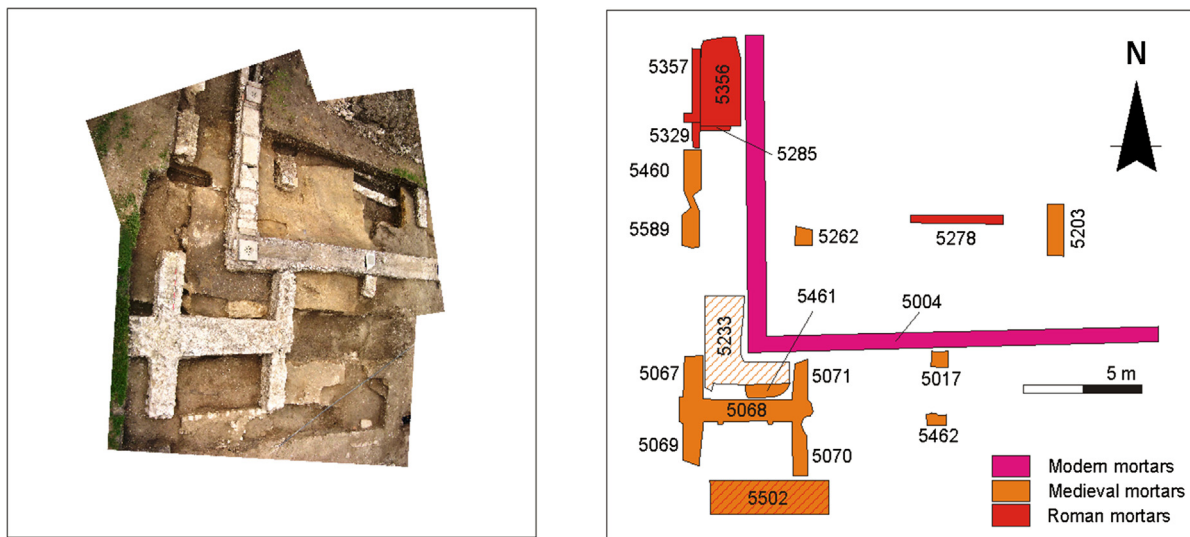
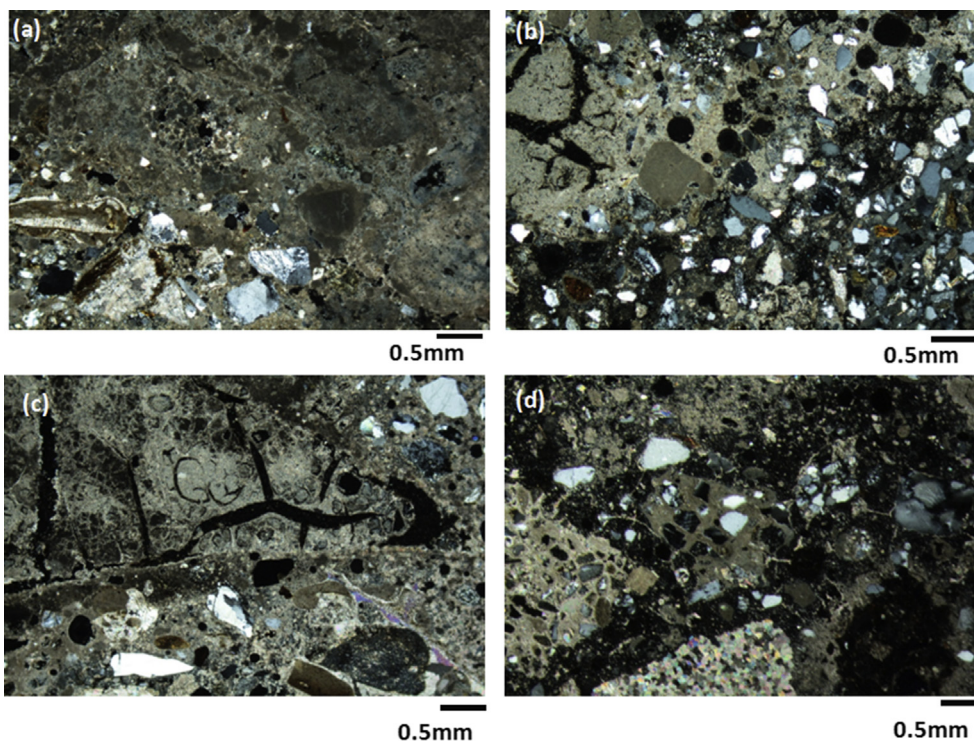**Fig. 1.** Overview of the excavated area (left) and sketch map with the remaining structures (right).

Fig. 2. Macroscopic pictures of some selected mortar surfaces. (a) 5004-35; (b) 5285-1; (c) 5068-16; (d) 5033-50.

schists and bricks) jointed by mortars.

The excavation works gave us the opportunity to perform a sampling campaign over the different discovered structures to study the construction phases, as well on an interesting area probably used to manufacture mortar mixing, in which many fragments of *Panchina* calcarenite were found.

The main aim of this paper is, therefore, to characterize mortars from the structures of both the Roman *domus* and the old Pisa's Cathedral in the Miracles Square (Italy), with a particular interest in determining the provenance of the raw materials and technologies used in a same area in different constructive periods.

2. Materials and methods

Forty-two mortars were sampled from the remains of both Roman *domus* and old Pisa's Cathedral, along with two samples from Modern structures.

Macroscopic and microscopic features of the samples were observed

Table 1

Macroscopic features of sampled mortars from Roman, Medieval and Modern structures, grouped according to preliminary studies reported in [43].

Structure	Sample	Type	Macroscopic features			
			Colour	Adhesion	Cohesion	Lumps
Roman mortars (domus)	5262-30	Bedding mortar	Whitish-grey	Low	Low	Present, < 2 mm
	5278-31	Bedding mortar	Whitish-grey	Low	Low	Present, < 2 mm
	5278-32	Bedding mortar	Whitish-grey	Low	Low	Present, < 2 mm
	5285-1	Aggregate-rich sample	Whitish-grey	Very low	Very low	Present, < 2 mm
	5285-2	Bedding mortar	Whitish-grey	Low	Low	Present, < 2 mm
	5285-3	Bedding mortar	Whitish-grey	Low	Low	Present, < 2 mm
	5329-8	Bedding mortar	Whitish-grey	Low	Low	Present, < 2 mm
	5329-8bis	Bedding mortar	Whitish-grey	Low	Low	Present, < 2 mm
	5356-5	Bedding mortar	Whitish-grey	Low	Low	Present, < 2 mm
	5357-4	Bedding mortar	Whitish-grey	Low	Low	Present, < 2 mm
	5462-24	Bedding mortar	Whitish-grey	Low	Low	Present, < 2 mm
	5462-25	Bedding mortar	Whitish-grey	Low	Low	Present, < 2 mm
	5502-19	Bedding mortar	Creamy-ligh brown	Low	Low	Present, < 2 mm
	5356-6	Pavement mortar	Dark brown	Low	Low	Rare, < 2 mm
	5356-7	Pavement mortar	Creamy-ligh brown	Low	Low	Present, < 2 mm
Medieval mortars (Old Pisa Cathedral)	5017-23	Bedding mortar	Creamy-ligh brown	Low	Low	Present, < 10 mm
	5067-12	Bedding mortar	Creamy-ligh brown	Low	Low	Present, < 10 mm
	5068-15	Bedding mortar	creamy-ligh brown	Low	Low	Abundant, < 10 mm
	5068-16	Bedding mortar	Creamy-ligh brown	Low	Low	Abundant, < 10 mm
	5068-200	Bedding mortar	Creamy-ligh brown	Low	Low	Abundant, < 10 mm
	5068-201	Bedding mortar	Creamy-ligh brown	Low	Low	Abundant, < 10 mm
	5068-202	Bedding mortar	Creamy-ligh brown	Low	Low	Abundant, < 10 mm
	5068-203	Bedding mortar	creamy-ligh brown	Low	Low	Abundant, < 10 mm
	5068-300	Bedding mortar	creamy-ligh brown	Low	Low	Abundant, < 10 mm
	5068-301	Bedding mortar	Creamy-ligh brown	Low	Low	Present, < 2 mm
	5068-302	Bedding mortar	Creamy-ligh brown	Low	Low	Abundant, < 10 mm
	5068-303	Bedding mortar	Creamy-ligh brown	Low	Low	Abundant, < 10 mm
	5069-13	Bedding mortar	Creamy-ligh brown	Low	Low	Abundant, < 10 mm
	5069-14	Bedding mortar	Creamy-ligh brown	Low	Low	Abundant, < 10 mm
	5070-17	Bedding mortar	Creamy-ligh brown	Low	Low	Abundant, < 10 mm
	5071-18	Bedding mortar	Creamy-ligh brown	Low	Low	Abundant, < 10 mm
	5203-33	Bedding mortar	Creamy-ligh brown	Low	Low	Abundant, < 10 mm
	5203-34	Bedding mortar	Creamy-ligh brown	Low	Low	Abundant, < 10 mm
	5460-9	Bedding mortar	Creamy-ligh brown	Low	Low	Abundant, < 10 mm
	5461-21	Bedding mortar	Creamy-ligh brown	Low	Low	Rare, < 2 mm
	5461-22	Bedding mortar	Creamy-ligh brown	Low	Low	Rare, < 2 mm
	5502-20	Bedding mortar	Creamy-ligh brown	Low	Low	Rare, < 2 mm
	5589-10	Bedding mortar	Creamy-ligh brown	Low	Low	Abundant, < 10 mm
	5589-11	Bedding mortar	Creamy-ligh brown	Low	Low	Abundant, < 10 mm
	5233-50	Binder-rich sample	Creamy	Low	Low	Absent
Modern mortars	5004-35	Bedding mortar	Creamy-ligh brown	Medium-low	High	Rare, < 2 mm
	5004-36	Bedding mortar	Creamy-ligh brown	Medium-low	High	Rare, < 2 mm

by a stereomicroscope (up to 200×) and by a polarising microscope working on polished thin sections. The quantitative mineralogical composition (vol.%) of the samples was performed through a point-counter (no less than 200 points) on polished thin sections.

The amounts of major and minor chemical components (Na_2O, MgO, Al_2O_3, SiO_2, P_2O_5, K_2O, CaO, TiO_2, MnO, Fe_2O_3) within the studied samples were determined by X-ray fluorescence (XRF) on pressed powder pellets utilizing an ARL 9400 XP + sequential X-ray spectrometer under the instrumental conditions reported by Lezzerini et al. [46]. Quantitative chemical data were obtained using correction for matrix effects based on international rock standards. The precision was monitored by routinely running a well-investigated in-house standards [47]. The accuracy, evaluated using international standards, ranges from 20% (MgO) to 1% (CaO), with a mean value of 5% for the other elements [46].

Thermogravimetric analysis (TGA) was used to evaluate the presence and the amount of volatile compounds (essentially H_2O, CO_2) in the samples. TGA were conducted in the range 110–1000 °C on about 25 mg of sample, dried (silica gel as drying agent) at room temperature for at least a week under the following experimental conditions: open alumina crucibles, heating rate of 10 °C/min and 30 ml/min nitrogen gas flow. The CO_2 content was also determined by a gasometric technique [48].

Qualitative mineralogical compositions of bulk mortar sample were performed by X-ray powder diffraction (XRPD). The experimental conditions were: Bragg-Brentano geometry, Ni-filtered CuK_α radiation obtained at 40 kV and 20 mA, 5–60 °2θ investigated range, 0.02° step, 2 s counting time per step. To identify the mineralogical phases in the X-ray spectra, a search/match approach DIFFRACPlus EVA) was used by comparing experimental peaks with PDF2 reference patterns.

Scanning electron microscope observations and micro-chemical compositions of both intergranular binder and lumps were performed using a SEM-EDS with 20 kV acceleration voltage, 0.1 nA beam current, and 100 s live time.
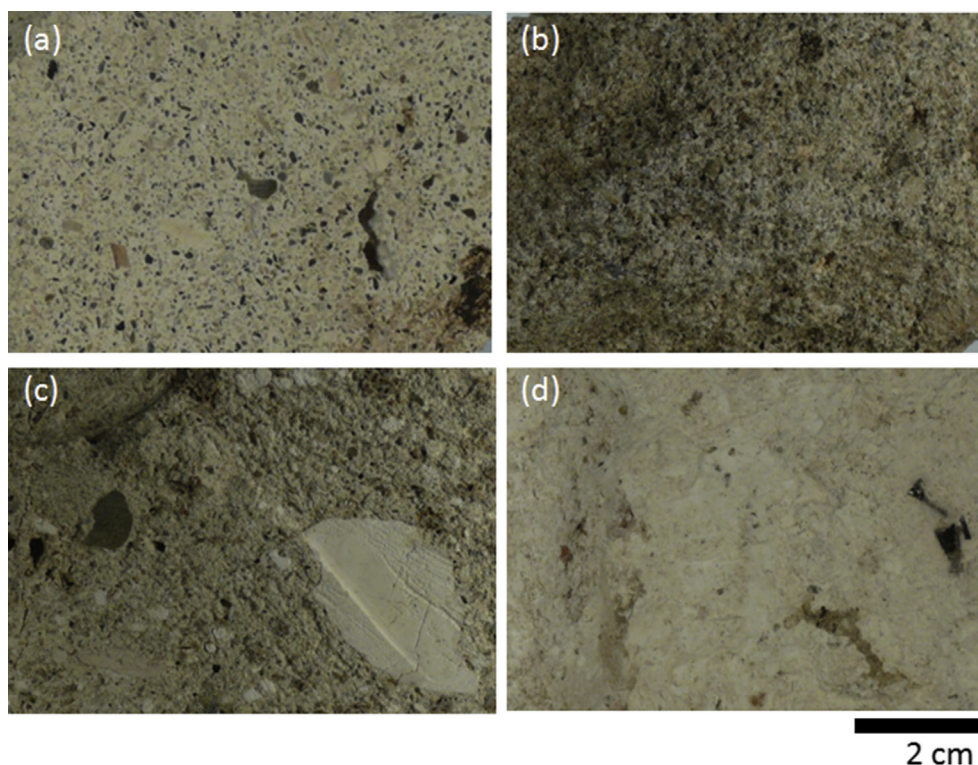
Fig. 3. Thin section microphotographs of some selected samples. (a) 5233-50 (lime putty sample); (b) 5068-303; (c) 5068-203; (d) 5203-34.

The chemical composition (including CO_2 and H_2O^+) and the weight percentages of both binder and aggregate were derived by combining the SEM/EDS data on the binder with modal aggregate composition and XRF bulk sample analyses as suggested by Franzini et al. [32].

The equation system describing the chemical composition of a mortar:

$$|(C_i)_m = Xa(C_i)_a + Xb(C_i)_b| \quad i = 1, ..., n \tag{1}$$

where the subscripts refer to mortar (m), aggregate (a) and binder (b), the C_i are the weight percentages of each chemical component, and Xa and Xb (with Xb = 1 – Xa) are the weight fractions of aggregate and binder, respectively, was solved by selecting the subset of equations relative to the H_2O, CO_2 and CaO components.

CaO(a) and CO_2(a) contents were estimated by the modal percentage of carbonates (almost entirely represented by calcite); the small amount of CaO(a) contained in the plagioclases of the aggregate was neglected. The H_2O(a) content was assumed as 0.5% for all samples (the only appreciable hydrated minerals in the aggregate are micas and chlorites, and their total amount is always below 10%.

Real density (ρ_s) was measured through an automatic He-pycnometer on ~10 g of very-fine-grained powders, dried at 105 ± 5 °C for 24hr, using these experimental conditions: ultrahigh purity compressed He, target pressure of 100 kPa; equilibrium time: automatic; purge mode: 3 min of continuous flow; maximum runs: 6; number of averaged runs: the last three. Apparent density (ρ_b) and open porosity (to water), which has been measured as water absorption at atmospheric pressure in respect to weight (Ab_w) or volume (Ab_v) of the specimens, were performed on samples with a volume of about 30 cm^3, as indicated by UNI 11060:2003 [49]. In particular, apparent density was calculated as the ratio between the mass of the dry sample and its volume, measured

by means of a hydrostatic balance on water-saturated samples [50]. Total porosity (P) and saturation index (SI) were calculated as follows: $P(\%) = 100 \cdot (1 - \rho_b/\rho_s)$ and $SI(\%) = 100 \cdot Ab_v/P$.

3. Results

Studied samples include thirty-eight bedding mortars, a sample mainly consisting in sandy aggregate (5285-1), two floor mortars characterized by limestone fragments (5356-7) and by limestone and cocciopesto fragments (5356-6), and a hardened lime putty (5233-50) (Fig. 2). The occurrence of a large amount of residual binder, sampled from a lime pit in correspondence of medieval structures (see Fig. 1) must be taken in great account, as its compositional features possible reflect the raw material employed in the manufacture process of Medieval mortars.

Overall, the adhesion of samples ranges from very low to low, while the cohesion is generally low; samples are, in fact, mainly friable and only in rare case tenacious. The aggregate grains range from silt (sample 5233-50) to gravel sized (samples 5356-6 and 5356-7). Color is from creamy-light brown (28 samples) to whitish-grey (12 samples), with the exception of the lime sample, that exhibits a creamy color. Lumps are widely present, with a grain size ranging from < 2 mm to < 10 mm. Details about macroscopic features of studied samples are reported in Table 1; mortars are listed according to groups and construction phases identified in a preliminary study by Lezzerini and Giubbilini reported in [43].

3.1. Mineralogical and petrographic data

The thin section analysis of studied mortars allows describing both

Table 2
Real density (ρ_s), apparent density (ρ_b), water absorption at atmospheric pressure in respect to weight (W_w) and volume (W_v), total porosity (P) and saturation index (SI) for the studied mortar samples.

Sample	ρ_s	ρ_b	W_w	W_v	P	SI
5262-30	2.60	1.46	29.40	42.98	43.8	98
5278-31	2.62	1.68	20.69	34.85	35.9	97
5278-32	2.62	1.68	20.84	35.01	35.9	98
5285-1	2.63	2.63	–	–	–	–
5285-2	2.60	1.60	23.33	37.40	38.5	97
5285-3	2.61	1.59	23.97	38.03	39.1	97
5329-8	2.61	1.74	18.54	32.30	33.3	97
5329-8bis	2.62	1.82	15.48	28.14	30.5	92
5356-5	2.62	1.62	21.43	34.79	38.2	91
5357-4	2.61	1.78	16.64	29.65	31.8	93
5462-24	2.61	1.68	19.91	33.51	35.6	94
5462-25	2.62	1.55	25.06	38.93	40.8	95
5502-19	2.62	1.50	26.65	39.87	42.7	93
5356-6	2.65	2.02	10.79	21.75	23.8	91
5356-7	2.66	2.05	9.96	20.41	22.9	89
5017-23	2.63	1.52	26.26	39.85	42.2	94
5067-12	2.65	1.40	31.74	44.47	47.2	94
5068-15	2.65	1.42	30.35	43.09	46.4	93
5068-16	2.65	1.38	32.62	45.05	47.9	94
5068-200	2.64	1.47	27.64	40.61	44.3	92
5068-201	2.64	1.38	31.95	43.98	47.7	92
5068-202	2.64	1.25	38.88	48.62	52.7	92
5068-203	2.65	1.44	28.90	41.72	45.7	91
5068-300	2.64	1.40	28.94	40.62	47.0	86
5068-301	2.63	1.54	25.94	40.00	41.4	97
5068-302	2.64	1.23	41.94	51.64	53.4	97
5068-303	2.64	1.47	28.81	42.38	44.3	96
5069-13	2.66	1.34	36.28	48.48	49.6	98
5069-14	2.63	1.40	31.50	43.99	46.8	94
5070-17	2.64	1.37	33.97	46.61	48.1	97
5071-18	2.63	1.45	28.77	41.64	44.9	93
5203-33	2.64	1.31	36.28	47.65	50.4	95
5203-34	2.64	1.18	44.86	53.14	55.3	96
5460-9	2.63	1.41	31.22	44.15	46.4	95
5461-21	2.63	1.38	33.13	45.73	47.5	96
5461-22	2.62	1.42	31.76	45.15	45.8	99
5502-20	2.65	1.59	23.60	37.57	40.0	94
5589-10	2.64	1.42	31.60	44.86	46.20	97
5589-11	2.64	1.32	36.45	48.27	50.00	97
5233-50	2.68	1.33	37.53	49.85	50.40	99
5004-35	2.61	1.59	22.59	35.98	39.10	92
5004-36	2.61	1.64	21.89	35.89	37.20	96

aggregate and binder features. Detailing, the aggregates exhibits a ranging grain size from medium (2–0.5 mm) to very fine (0.25–0.125 mm); they exhibit a medium-high sphericity, from sub-angular to sub-rounded shape. From the mineralogical point of view, the aggregate consists of quartz, feldspars, rock fragments including also limestones and *Panchina* calcarenite, calcite fragments, phyllosilicates e rare garnet, epidote, tourmaline and zircon. The binder shows an overall non-homogeneous texture, due to the presence of lumps and underburned fragments attributable to *Panchina* calcarenite. Lumps range from present to rare, with dimension from 2 to 10 mm. Microphotographs of some representative samples are reported in Fig. 3. Overall, despite slight differences in term of binder/aggregate ratio, the binder characteristics and the mineralogical composition of aggregates are quite similar in all studied samples.

3.2. Physical proprieties

In Table 2, the measured and calculated main physical proprieties of the studied mortars are reported. The collected data reveals a quite

homogeneous value in real density (on average $2.63 \pm 0.02 \, \text{g/cm}^3$), with the exception of the binder-rich sample 5233-50, characterized by very low content of aggregate. The highest value of apparent density is reported for sample 5285-1, due to mainly aggregate fraction present. Overall, all the studied mortar samples exhibit a wide range of values for water absorption (W_w, W_v), porosity (P) and saturation index (SI), with the exception of floor mortars (5356-6 and 5356-7), for which the lower values of the measured parameters were calculated. Noteworthy, no correlation between construction phases and physical proprieties can be highlighted.

3.3. Chemical data

The chemical composition of the studied mortars obtained through XRF analysis on the whole sample is reported in Table 3. Based on the obtained data, a slightly different composition can be assessed for mortars sampled from Roman and Medieval structures, as well from Modern ones.

Detailing, Roman mortars, along with the two specimens sampled from modern structures, exhibit the highest content in SiO_2 (on average $47 \pm 19 \, \text{wt\%}$ and $46 \pm 4 \, \text{wt\%}$, respectively), Al_2O_3 (on average $6 \pm 2 \, \text{wt\%}$ and $6.9 \pm 0.6 \, \text{wt\%}$) and Fe_2O_3 (on average $2.4 \pm 0.6 \, \text{wt\%}$ and $2.1 \pm 0.1 \, \text{wt\%}$), and the lowest levels in CaO (on average $23 \pm 12 \, \text{wt\%}$ and $24 \pm 3 \, \text{wt\%}$). On the contrary, mortars sampled from Medieval structures exhibit the highest content in CaO (on average $39 \pm 4 \, \text{wt\%}$), and the lowest content in SiO_2 (on average $22 \pm 5 \, \text{wt\%}$), Al_2O_3 (on average $4.0 \pm 0.8 \, \text{wt\%}$), and Fe_2O_3 (on average $1.5 \pm 0.3 \, \text{wt\%}$).

Finally, as regard water, the high content computed from the analyses (on average about 4 wt%) cannot be attribute to the solely aggregate, so that has to be assumed that the greater contribute is due to the binder fraction.

It has to be noticed that chemical data by XRF are referred to the whole samples, accounting the contribution of both aggregates and binder. In this prospective, a better discrimination between the possible different features in mortars manufacture can be reached by in-deep analysis on the solely binder fraction.

3.4. The binder

Chemical data collected by SEM-EDS on both intergranular binder and lumps (Table 4) reveal, an overall, the employment of a hydraulic lime (Fig. 4). However, the elemental composition indicates a slightly change in receipt over the different construction phases.

In detail, mortar samples from Roman and Modern structures report a low percentage of binder (on average $34 \pm 9\%$ and $47 \pm 5\%$, respectively), while in the Medieval mortars a high percentage of binder was calculated ($63 \pm 11\%$). The binder composition reflects data obtained on the whole samples by XRF analysis, revealing a calcium-rich composition in Medieval mortars, which also however exhibit the higher level in SiO_2 in the binder fraction ($5.0 \pm 1.5 \, \text{wt\%}$) than Roman and Modern ones ($3.4 \pm 1.0 \, \text{wt\%}$ and $4.5 \pm 1.0 \, \text{wt\%}$). Of course, exceptions are represented by samples 5285-1 and 5233-50, consisting quite exclusively of aggregate and binder fraction, respectively.

This result could appear in contrast with chemical data obtained on the whole samples by XRF, indicating the Roman mortars as enriched in SiO_2, Al_2O_3 and Fe_2O_3.

However, a carefully inspection of the graph $CaO-H_2O-(SiO_2 + Al_2O_3 + Fe_2O_3)$, in which the stability field of CSH systems proposed by Taylor [51] were also reported (Fig. 5), indicates that in Medieval mortars the non-carbonate amorphous phase is quite exclusively due to CSH (I) phases, thus attributable to the binder fraction.

Table 3

Chemical composition (wt%) obtained by XRF analysis and CaO excess to form calcite (ΔCaO). Volatile compounds (H_2O and CO_2) were determined by thermo-gravimetric analysis (TGA).

Structure	Sample	H_2O	CO_2	Na_2O	MgO	Al_2O_3	SiO_2	P_2O_5	K_2O	CaO	TiO_2	MnO	Fe_2O_3	SiO_2 + CaO	ΔCaO
Roman mortars (domus)	5262-30	3.19	10.71	1.17	1.49	8.18	48.85	0.13	1.53	22.47	0.15	0.07	2.06	71.32	8.84
	5278-31	2.77	12.98	1.09	1.32	6.08	48.70	0.22	0.98	23.20	0.21	0.08	2.37	71.90	6.68
	5278-32	2.21	11.86	1.22	1.41	6.76	50.72	0.21	1.14	21.70	0.22	0.03	2.52	72.42	6.61
	5285-1	1.90	0.31	2.23	0.80	8.77	81.55	0.03	1.70	1.11	0.29	0.01	1.30	82.66	0.72
	5285-2	2.62	10.78	1.12	1.48	6.30	50.74	0.23	1.21	22.07	0.25	0.12	3.08	72.81	8.35
	5285-3	2.72	8.46	1.23	1.42	6.97	58.40	0.20	1.19	16.14	0.24	0.10	2.93	74.54	5.37
	5329-8	3.22	11.96	1.02	1.91	6.38	49.52	0.20	0.99	21.49	0.25	0.09	2.97	71.01	6.27
	5329-8bis	3.46	11.97	1.04	2.28	6.19	49.35	0.19	0.96	21.43	0.24	0.08	2.81	70.78	6.20
	5356-5	2.56	10.28	1.30	1.33	6.62	55.36	0.22	1.10	18.03	0.23	0.10	2.87	73.39	4.95
	5357-4	2.18	11.66	1.01	1.47	6.50	49.41	0.27	1.12	22.98	0.25	0.09	3.06	72.39	8.14
	5462-24	3.01	16.61	0.83	1.65	5.99	40.33	0.45	0.91	27.60	0.20	0.08	2.34	67.93	6.46
	5462-25	5.28	9.61	1.13	2.03	6.94	55.10	0.25	0.99	15.84	0.23	0.08	2.52	70.94	3.61
	5502-19	4.73	11.79	1.44	1.75	7.87	50.65	0.19	1.38	18.03	0.18	0.05	1.94	68.68	3.02
	5356-6	5.57	33.53	0.15	0.70	3.41	7.55	0.44	0.47	46.20	0.14	0.05	1.79	53.75	3.54
	5356-7	2.70	36.29	0.10	0.59	2.27	5.80	0.32	0.49	50.11	0.09	0.04	1.20	55.91	3.93
Medieval mortars (Old Pisa Cathedral)	5017-23	3.32	24.27	0.40	3.18	4.35	21.62	0.19	0.69	40.07	0.12	0.06	1.73	61.69	9.19
	5067-12	5.12	24.45	0.29	6.64	4.08	21.87	0.00	0.54	35.37	0.10	0.06	1.48	57.24	4.26
	5068-15	5.80	25.47	0.25	4.24	3.60	22.05	0.13	0.47	36.48	0.09	0.05	1.37	58.53	4.07
	5068-16	4.99	25.84	0.27	4.90	3.70	21.16	0.09	0.44	37.11	0.09	0.05	1.35	58.27	4.22
	5068-200	5.11	23.82	0.25	5.67	4.42	22.77	0.16	0.52	35.56	0.10	0.06	1.56	58.33	5.24
	5068-201	4.92	22.90	0.33	4.69	4.45	26.71	0.16	0.60	33.49	0.11	0.06	1.58	60.20	4.34
	5068-202	5.48	25.31	0.36	1.35	4.13	23.95	0.15	0.57	37.02	0.10	0.06	1.52	60.97	4.82
	5068-203	6.66	25.18	0.16	6.24	3.60	21.37	0.10	0.36	34.92	0.08	0.05	1.28	56.29	2.86
	5068-300	6.69	24.77	0.19	5.09	3.80	22.09	0.13	0.44	35.32	0.08	0.06	1.34	57.41	3.78
	5068-301	4.28	21.70	0.44	4.08	4.85	28.44	0.21	0.69	33.33	0.12	0.07	1.79	61.77	5.71
	5068-302	4.03	24.64	0.44	2.90	4.13	24.11	0.19	0.61	37.26	0.10	0.05	1.54	61.37	5.90
	5068-303	4.20	24.51	0.34	3.93	4.47	22.99	0.15	0.55	37.11	0.10	0.06	1.59	60.10	5.90
	5069-13	2.35	30.56	0.37	1.43	2.89	15.90	0.03	0.54	44.65	0.08	0.04	1.16	60.55	5.76
	5069-14	4.84	24.97	0.30	2.49	4.31	20.97	0.05	0.56	39.65	0.11	0.06	1.69	60.62	7.88
	5070-17	4.56	26.67	0.32	3.34	3.69	18.68	0.04	0.52	40.39	0.10	0.06	1.63	59.07	6.46
	5071-18	4.57	24.03	0.35	3.91	4.21	20.68	0.04	0.64	39.56	0.12	0.07	1.82	60.24	8.99
	5203-33	5.49	26.43	0.24	1.37	3.93	21.59	0.02	0.36	38.92	0.09	0.05	1.51	60.51	5.28
	5203-34	5.01	27.20	0.14	1.30	3.67	18.58	0.03	0.34	42.15	0.09	0.05	1.44	60.73	7.54
	5460-9	4.10	23.90	0.35	1.68	5.22	25.19	0.06	0.71	36.99	0.11	0.06	1.63	62.18	6.57
	5461-21	2.24	23.85	0.67	1.08	4.23	25.10	0.16	0.84	39.97	0.11	0.07	1.68	65.07	9.63
	5461-22	2.48	23.89	0.54	1.08	4.03	22.61	0.19	0.81	42.24	0.11	0.07	1.95	64.85	11.84
	5502-20	3.64	26.57	0.30	1.73	4.37	23.65	0.17	0.57	37.29	0.13	0.05	1.53	60.94	3.48
	5589-10	3.17	26.85	0.52	1.14	3.85	19.80	0.14	0.73	42.15	0.10	0.05	1.50	61.95	8.00
	5589-11	5.10	25.02	0.48	1.29	4.48	24.95	0.14	0.71	36.12	0.10	0.06	1.55	61.07	4.28
	5233-50	5.40	38.92	0.04	0.94	0.58	2.62	0.09	0.09	50.92	0.02	0.02	0.36	53.54	1.40
Modern mortars	5004-35	4.97	13.89	0.67	2.16	6.42	43.07	0.10	1.06	25.45	0.14	0.08	1.99	68.52	7.77
	5004-36	3.00	12.12	1.11	1.64	7.33	49.02	0.12	1.42	21.86	0.15	0.08	2.15	70.88	6.43

On the contrary, the other mortars seem to exhibit a water deficit in respect to CSH phases. The computed normative analysis reporting the chemical composition of carbonate and non-carbonate amorphous fraction of the binder calculated according to Franzini et al. [32] is reported in Table 5.

3.5. The aggregate

The preliminary minero-petrographic analysis of the studied samples allowed obtaining valuable information of aggregate fraction, mainly due to quartz, feldspars and rock fragments, including also limestones, calcarenites (mainly *Panchina* fragments), and small amount of marbles. To go deeper inside the composition of aggregates and try to obtain provenance information on raw materials employed in mortar manufacture, chemical composition of aggregates and aggregate percentage (%) were also calculated as suggested by Franzini et al. [32] for the aggregate fractions. The obtained results, reported in Table 6, are quite in accordance with previous data obtained on both whole sample and binder fraction. In fact, Roman and Modern mortars reveal the highest percentage of aggregate (66 ± 9% and 53 ± 5%, respectively, on average), while in the Medieval mortars the lowest percentage of aggregate was calculated (average value 38 ± 11%). As regard composition, effectively, the aggregate fraction in Roman mortars exhibit a slightly SiO_2-rich composition (43 ± 19 wt%), matching the results obtained by both XRF analysis and recalculated normative composition of binder (see Fig. 4).

4. Discussion and conclusions

Following the aims of this study, finalized to characterize mortars from the Pisa's Cathedral Square, and in particular from structures oldest than the well-known Medieval complex, the following consideration can be provided.

The most relevant observation regards the presence of *Panchina* calcarenite, occurring in almost all samples as underburned fragments; this evidence suggests interesting implication in the evaluation of

Table 4
Chemical composition of binders and binder percentage (%), calculated as suggested by Franzini et al. [32].

| Sample	H$_2$O	CO$_2$	MgO	Al$_2$O$_3$	SiO$_2$	CaO	Fe$_2$O$_3$	Binder%
5262-30	2.89	7.62	0.74	4.19	5.17	18.54	0.89	40.04
5278-31	2.45	8.77	0.29	2.45	3.53	17.84	1.41	36.74
5278-32	1.89	8.44	0.43	3.06	3.68	17.33	1.86	36.69
5285-1	1.44	0.31	0.29	3.28	0.54	1.11	1.07	8.04
5285-2	2.33	10.30	0.24	2.39	4.38	21.46	1.44	42.54
5285-3	2.39	7.79	0.52	2.41	2.94	15.28	2.28	33.61
5329-8	2.92	10.32	0.67	2.08	3.55	19.40	1.84	40.78
5329-8bis	3.17	10.49	0.83	2.32	3.71	19.54	1.69	41.75
5356-5	2.25	9.45	0.59	2.90	2.91	16.98	2.25	37.33
5357-4	1.88	9.27	0.04	2.63	4.05	19.93	1.78	39.58
5462-24	2.65	4.83	0.02	2.62	3.49	12.59	0.86	27.06
5462-25	4.91	3.71	1.32	3.14	2.86	8.33	1.69	25.96
5502-19	4.36	3.36	1.34	5.01	3.23	7.29	1.75	26.34
5356-6	5.27	9.83	0.22	3.16	3.15	16.01	1.78	39.42
5356-7	2.39	11.06	0.08	1.79	3.49	17.98	1.05	37.84
5017-23	3.13	16.03	2.67	2.60	7.26	29.58	0.74	62.01
5067-12	4.98	20.25	6.62	2.12	7.62	30.02	1.11	72.72
5068-15	5.62	18.17	4.15	2.88	6.17	27.18	0.44	64.61
5068-16	4.80	18.32	4.13	1.47	5.59	27.53	0.19	62.03
5068-200	4.90	15.15	4.34	2.55	6.00	24.50	0.61	58.05
5068-201	4.75	19.29	4.04	2.44	5.53	28.89	0.90	65.84
5068-202	5.29	19.97	0.57	2.55	3.48	30.23	0.12	62.21
5068-203	6.38	10.89	4.07	1.61	4.65	16.70	0.09	44.39
5068-300	6.51	17.66	4.37	2.04	5.91	26.24	0.45	63.18
5068-301	3.99	10.85	2.42	0.54	3.91	19.51	0.64	41.86
5068-302	3.88	21.51	2.44	2.43	5.22	33.27	0.98	69.73
5068-303	4.02	17.88	3.34	2.98	5.95	28.64	1.24	64.05
5069-13	2.13	18.29	0.77	1.12	3.40	29.01	0.52	55.24
5069-14	4.70	20.19	2.09	3.07	6.08	33.57	1.26	70.96
5070-17	4.36	17.10	3.06	0.46	5.88	28.20	0.29	59.35
5071-18	4.34	12.43	3.21	2.35	6.86	24.79	0.88	54.86
5203-33	5.31	21.11	0.00	2.16	3.32	32.14	0.27	64.31
5203-34	4.83	19.48	0.27	2.32	4.55	32.32	0.42	64.19
5460-9	3.85	13.18	1.31	3.24	4.04	23.33	1.24	50.19
5461-21	2.04	17.04	0.95	2.22	5.84	31.30	1.22	60.61
5461-22	2.35	21.57	0.47	1.84	6.38	39.29	1.48	73.38
5502-20	3.45	21.21	0.92	2.66	2.77	30.47	0.58	62.06
5589-10	2.95	16.58	0.63	1.70	4.18	29.08	0.93	56.05
5589-11	4.92	20.77	1.02	2.56	3.22	30.70	0.75	63.94
5233-50	5.39	38.69	0.86	0.29	1.74	50.64	0.28	97.89
5004-35	4.72	11.71	1.72	3.12	5.20	22.67	1.26	50.40
5004-36	2.71	10.89	0.76	3.29	3.84	20.29	1.28	43.06
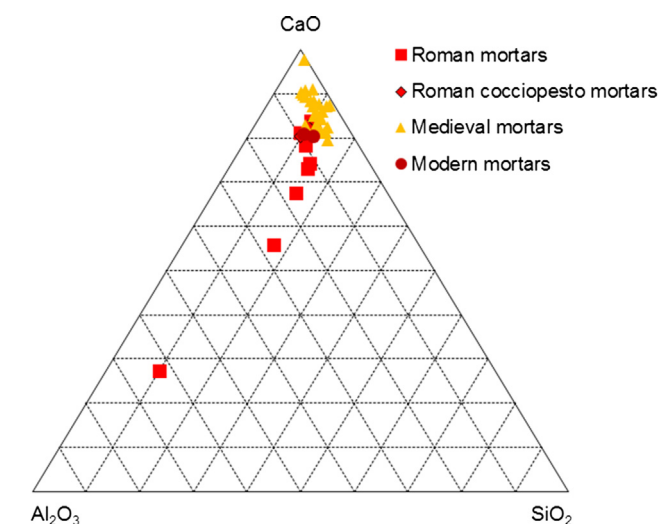
Fig. 4. Triangular diagram CaO-Al$_2$O$_3$-SiO$_2$ describing the binder composition based on computed normative analysis.
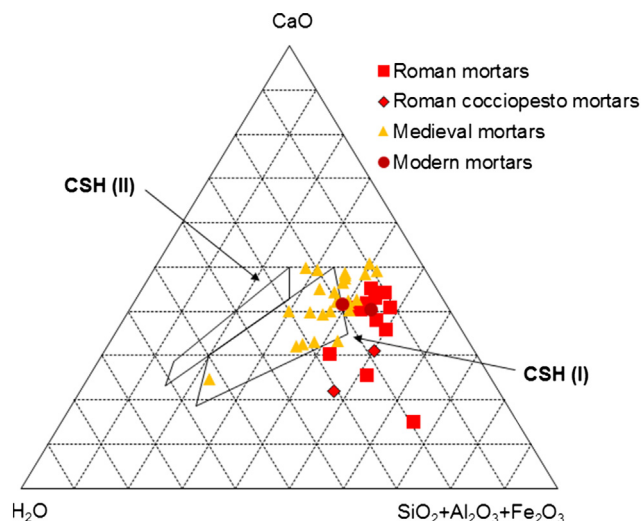

Fig. 5. Triangular diagram CaO-H$_2$O-(SiO$_2$ + Al$_2$O$_3$ + Fe$_2$O$_3$) in which the chemical composition of the binder amorphous phase calculated on the basis of SEM-EDS data are plotted. CSH (I) and CSH (II) compositional variation fields are from [51].

manufacture process employed to realize the studied mortars, as well on the technological level of artisans working on the construction of both Roman *domus* and the successive old Pisa's Cathedral. Despite the slight differences highlighted between Roman and Medieval mortars, an overall homogenous composition can be attributed to all the studied samples, with a variability mainly regarding the aggregate/binder ratio (namely higher binder% in Medieval mortars than in Roman ones, and more quartz-rich aggregates in Roman mortars).

Going to inspect raw materials provenance issues, by comparing the calculated chemical composition obtained on the binder fraction with possible calcite-based materials available to manufacture mortars (Fig. 6), studied samples are plotted in the compositional range of *Panchina* calcarenite; outliers respect to the defined trend are samples 5285-1 and 5233-50, consisting respectively in an aggregate-rich and a lime-rich specimen. It is interesting to note that sample 5233-50 shows a good compositional match with *Monte Pisano* marble, a building material that will be largely quarried and employed for both buildings and mortars manufacture up to the 11th century, during the construction of the Medieval Pisa Cathedral and the entire complex in Miracle Square [44]. Thus, in the aforementioned structures, high quality hydraulic mortars were obtained by burning *Monte Pisano* marble and adding diatomite to the mixture [2]. However, the low technical proprieties of studied mortars (low adhesion and cohesion, medium hydraulicity), as well the occurrence of *Panchina* calcarenite fragments and the relatively low exploitation of *Monte Pisano* marble during Roman and early Medieval Age, lead to exclude a similar manufacture recipe. A possible hypothesis encompasses the use of mixed carbonate source, obtained by burning sporadic marble blocks (obtained as building scraps) and *Panchina* calcarenite; effectively, has to be noticed that before the 11th century this stone was largely employed in civil and religious structures, as well in the structures from which mortars were sampled.

Finally, as regard aggregates, by comparing the mineralogical data obtained by optical microscopy observations of thin sections with Serchio and Arno River sands along with *Panchina* calcarenite (Fig. 7), the obtained results clearly show that all the studied samples are plotted in a compositional range consisting of the all reference

Table 5

Average computed normative analysis of the intergranular binder and lumps, and chemical composition of amorphous phases for each identified group of studied mortars, calculated as suggested by Franzini et al. [32].

Group	Normative analysis				Composition (wt%) of amorphous phase				
		Calcite	Magnesite	Amorphous phase	H_2O	Al_2O_3	SiO_2	CaO	Fe_2O_3
Group 1 - Roman mortars	Average	43.54	3.6	52.86	17.21	18.04	19.56	35.55	9.65
	St.dev.	17.9	3.44	15.24	5.87	8.01	4.42	8.93	2.98
Group 2 - Medieval mortars	Average	56.9	8.14	34.96	21.64	9.88	23.16	42.03	3.29
	St.dev.	13.64	5.97	8.74	8.97	4	2.71	6.74	1.67
Group 3 - Modern mortars	Average	48.75	5.42	45.84	16.96	15.23	20.95	40.84	6.03
	St.dev.	6.22	2.45	3.77	3.34	3.49	0.44	0.95	1.24

Table 6

Chemical composition of aggregates and aggregate percentage (%), calculated as suggested by Franzini et al. [32].

Sample	H_2O	CO_2	Na_2O	MgO	Al_2O_3	SiO_2	P_2O_5	K_2O	CaO	TiO_2	MnO	Fe_2O_3	Aggregate%
5262-30	0.30	3.09	1.17	0.75	3.99	43.68	0.13	1.53	3.93	0.15	0.07	1.17	59.96
5278-31	0.32	4.21	1.09	1.03	3.63	45.17	0.22	0.98	5.36	0.21	0.08	0.96	63.26
5278-32	0.32	3.42	1.22	0.98	3.70	47.04	0.21	1.14	4.37	0.22	0.03	0.66	63.31
5285-1	0.46	–	2.23	0.51	5.49	81.01	0.03	1.70	–	0.29	0.01	0.23	91.96
5285-2	0.29	0.48	1.12	1.24	3.91	46.36	0.23	1.21	0.61	0.25	0.12	1.64	57.46
5285-3	0.33	0.67	1.23	0.90	4.56	55.46	0.20	1.19	0.86	0.24	0.10	0.65	66.39
5329-8	0.30	1.64	1.02	1.24	4.30	45.97	0.20	0.99	2.09	0.25	0.09	1.13	59.22
5329-8bis	0.29	1.48	1.04	1.45	3.87	45.64	0.19	0.96	1.89	0.24	0.08	1.12	58.25
5356-5	0.31	0.83	1.30	0.74	3.72	52.45	0.22	1.10	1.05	0.23	0.10	0.62	62.67
5357-4	0.30	2.39	1.01	1.43	3.87	45.36	0.27	1.12	3.05	0.25	0.09	1.28	60.42
5462-24	0.36	11.78	0.83	1.63	3.37	36.84	0.45	0.91	15.01	0.20	0.08	1.48	72.94
5462-25	0.37	5.90	1.13	0.71	3.80	52.24	0.25	0.99	7.51	0.23	0.08	0.83	74.04
5502-19	0.37	8.43	1.44	0.41	2.86	47.42	0.19	1.38	10.74	0.18	0.05	0.19	73.66
5356-6	0.30	23.70	0.15	0.48	0.25	4.40	0.44	0.47	30.19	0.14	0.05	0.01	60.58
5356-7	0.31	25.23	0.10	0.51	0.48	2.31	0.32	0.49	32.13	0.09	0.04	0.15	62.16
5017-23	0.19	8.24	0.40	0.51	1.75	14.36	0.19	0.69	10.49	0.12	0.06	0.99	37.99
5067-12	0.14	4.20	0.29	0.02	1.96	14.25	0.00	0.54	5.35	0.10	0.06	0.37	27.28
5068-15	0.18	7.30	0.25	0.09	0.72	15.88	0.13	0.47	9.30	0.09	0.05	0.93	35.39
5068-16	0.19	7.52	0.27	0.77	2.23	15.57	0.09	0.44	9.58	0.09	0.06	1.16	37.97
5068-200	0.21	8.67	0.25	1.33	1.87	16.77	0.16	0.52	11.06	0.10	0.06	0.95	41.95
5068-201	0.17	3.61	0.33	0.65	2.01	21.18	0.16	0.60	4.60	0.11	0.06	0.68	34.16
5068-202	0.19	5.34	0.36	0.78	1.58	20.47	0.15	0.57	6.79	0.10	0.06	1.40	37.79
5068-203	0.28	14.29	0.16	2.17	1.99	16.72	0.10	0.36	18.22	0.08	0.05	1.19	55.61
5068-300	0.18	7.11	0.19	0.72	1.76	16.18	0.13	0.44	9.08	0.08	0.06	0.89	36.82
5068-301	0.29	10.85	0.44	1.66	4.31	24.53	0.21	0.69	13.82	0.12	0.07	1.15	58.14
5068-302	0.15	3.13	0.44	0.46	1.70	18.89	0.19	0.61	3.99	0.10	0.05	0.56	30.27
5068-303	0.18	6.63	0.34	0.59	1.49	17.04	0.15	0.55	8.47	0.10	0.06	0.35	35.95
5069-13	0.22	12.27	0.37	0.66	1.77	12.50	0.03	0.54	15.64	0.08	0.04	0.64	44.76
5069-14	0.14	4.78	0.30	0.40	1.24	14.89	0.05	0.56	6.08	0.11	0.06	0.43	29.04
5070-17	0.20	9.57	0.32	0.28	3.23	12.80	0.04	0.52	12.19	0.10	0.06	1.34	40.65
5071-18	0.23	11.60	0.35	0.70	1.86	13.82	0.04	0.64	14.77	0.12	0.07	0.94	45.14
5203-33	0.18	5.32	0.24	1.37	1.77	18.27	0.02	0.36	6.78	0.09	0.05	1.24	35.69
5203-34	0.18	7.72	0.14	1.03	1.35	14.03	0.03	0.34	9.83	0.09	0.05	1.02	35.81
5460-9	0.25	10.72	0.35	0.37	1.98	21.15	0.06	0.71	13.66	0.11	0.06	0.39	49.81
5461-21	0.20	6.81	0.67	0.13	2.01	19.26	0.16	0.84	8.67	0.11	0.07	0.46	39.39
5461-22	0.13	2.32	0.54	0.61	2.19	16.23	0.19	0.81	2.95	0.11	0.07	0.47	26.62
5502-20	0.19	5.36	0.30	0.81	1.71	20.88	0.17	0.57	6.82	0.13	0.05	0.95	37.94
5589-10	0.22	10.27	0.52	0.51	2.15	15.62	0.14	0.73	13.07	0.10	0.05	0.57	43.95
5589-11	0.18	4.25	0.48	0.27	1.92	21.73	0.14	0.71	5.42	0.10	0.06	0.80	36.06
5233-50	0.01	0.23	0.04	0.08	0.29	0.88	0.09	0.09	0.28	0.02	0.02	0.08	2.11
5004-35	0.25	2.18	0.67	0.44	3.30	37.87	0.10	1.06	2.78	0.14	0.08	0.73	49.60
5004-36	0.29	1.23	1.11	0.88	4.04	45.18	0.12	1.42	1.57	0.15	0.08	0.87	56.94

materials. This result should not surprise; in fact, in ancient time, Serchio was an Arno tributary, so that the possible availability of mixed alluvium has to be considered. Effectively, excluding the occurrence of *Panchina* calcarenite, quite similar results were obtained in studies performed on mortars from Pisa's Tower.

With these drawbacks, we can speculate that before 11th century, namely the construction of Miracle square complex, *Monte Pisano* marble was scarcely exploited so that only few blocks were available as building material; on the contrary, *Panchina* calcarenite was widely diffused in urban architecture. Thus, both Romans and artisans working

on the construction of old Cathedral possibly employed this stone to produce lime for mortar manufacture, with a slight change in technological level over the time. This is evidenced by the differences in aggregate/binder ratio and binder features between Roman and Medieval mortars, even if a quite homogeneity in raw materials use can be assessed.

Only after the massive marble exploitation from *Monte Pisano* since 11th century, the local marble will be used to produce lime, by the addition of diatomite, and Arno and Serchio River sands, the latter ones already employed in mortars since Roman age.
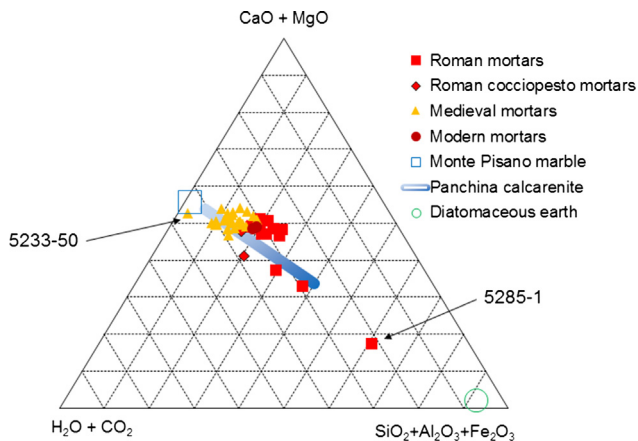
Fig. 6. Chemical composition of the whole binder compared with materials probably employed for its preparation (wt%).
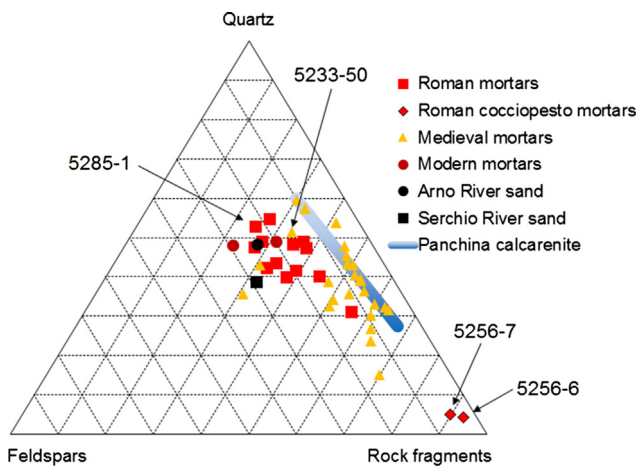

Fig. 7. Mineralogy of the aggregates compared with materials probably employed for mortar preparation (wt%).

References

[1] A. Moropoulou, A. Bakolas, K. Bisbikou, Investigation of the technology of historic mortars, J. Cult. Heritage 1 (2000) 45–58.
[2] M. Franzini, L. Leoni, M. Lezzerini, F. Sartori, The mortar of the "Leaning Tower" of Pisa: the product of a medieval technique for preparing high-strength mortars, Eur. J. Mineral. 12 (2000) 1151–1163.
[3] M.P. Riccardi, M. Lezzerini, F. Carò, M. Franzini, B. Messiga, Microtextural and microchemical studies of hydraulic ancient mortars: two analytical approaches to understand pre-industrial technology processes, J. Cult. Heritage 8 (2007) 350–360.
[4] S. Pavia, S. Caro, An investigation of Roman mortar technology through the petrographic analysis of archaeological material, Constr. Build. Mater. 22 (2008) 1807–1811.
[5] L. Bertolini, M. Carsana, M. Gastaldi, F. Lollini, E. Redaelli, Binder characterization of mortars used at different ages in the San Lorenzo church in Milan, Mater. Charact. 80 (2013) 9–20.
[6] G. Gallello, M. Ramacciotti, M. Lezzerini, E. Hernandez, M. Calvo, A. Morales, A. Pastor, M. De la Guardia, Indirect chronology method employing Rare Earth Elements to identify Sagunto Castle mortar construction periods, Microchem. J. 132 (2017) 251–261.
[7] M. Miriello, D. Barca, A. Bloise, A. Ciarallo, G.M. Crisci, T. De Rose, C. Garruso, F. Gazineo, M.F. La Russa, Characterization of archaeological mortars from Pompeii (Campania, Italy) and identification of construction phases by compositional data

[8] C. Corti, L. Rampazzi, R. Bugini, A. Sansonetti, M. Biraghi, L. Castelletti, I. Nobile, C. Orsenigo, Thermal analysis and archaeological chronology: the ancient mortars of the site of Baradello (Como, Italy), Thermochim. Acta 572 (2013) 71–84.
[9] R. Agostino, G. Barone, P. Mazzoleni, S. Raneri, G. Sabatino, M.M. Sica, Mortars and plasters from the Bruttii - Roman city of Tauriana (Palmi - RC) - preliminary data, Periodico di Mineralogia 82 (2013) 489–501.
[10] G. Biscontin, M. Pellizon Birelli, E. Zendri, Characterization of binders employed in the manufacture of Venetian historical mortars, J. Cult. Herit. 3 (2002) 31–37.
[11] F. Carò, M.P. Riccardi, M.T. Mazzilli Savini, Characterization of plasters and mortars as a tool in archaeological studies: the case of Lardirago castle in Pavia, Northern Italy, Archaeometry 50 (2008) 85–100.
[12] D. Miriello, A. Bloise, G.M. Crisci, C. Apollaro, A. La Marca, Characterization of archaeological mortars and plasters from Kyme (Turkey), J. Archaeol. Sci. 38 (2011) 794–804.
[13] D. Miriello, D. Barca, G.M. Crisci, L. Barba, J. Blancas, A. Ortiz, A. Pecci, L. Lopez, Luján, Characterization and provenance of lime plasters from the Templo Mayor of Tenochtitlan (Mexico City), Archaeometry 53 (2011) 1119–1141.
[14] D. Miriello, D. Barca, A. Pecci, R. De Luca, G.M. Crisci, Plasters from different buildings of the sacred precinct of Tenochtitlan (Mexico City): characterization and provenance, Archaeometry 57 (1) (2015) 100–127.
[15] M. Lezzerini, S. Legnaioli, G. Lorenzetti, V. Palleschi, M. Tamponi, Characterization of historical mortars from the bell tower of St. Nicholas church (Pisa, Italy), Construct. Build. Mater. 69 (2014) 203–212.
[16] F. Casadio, G. Chiari, S. Simon, Evaluation of binder/aggregate ratios in archaeological lime mortars with carbonate aggregate: a comparative assessment of chemical, mechanical and microscopic approaches, Archaeometry 47 (2005) 671–689.
[17] E. Gotti, J.P. Oleson, L. Bottalico, C. Brandon, R. Cucitore, R.L. Hohlfelder, A comparison of the chemical and engineering characteristics of ancient roman hydraulic concrete with a modern reproduction of vitruvian hydraulic concrete, Archaeometry 50 (2008) 576–590.
[18] D. Miriello, M. Lezzerini, F. Chiaravalloti, A. Bloise, C. Apollaro, G.M. Crisci, Replicating the chemical composition of the binder for restoration of historic mortars as an optimization problem, Comput. Concr. 12 (2013) 553–563.
[19] G. Chiari, G. Torraca, M.L. Santarelli, Recommendations for Systematic Instrumental Analysis of Ancient Mortars: The Italian Experience, STP1258, http://doi.org/10.1520/STP15442S.
[20] M. Franzini, L. Leoni, M. Lezzerini, F. Sartori, On the binder of some ancient mortars, Mineral. Petrol. 67 (1999) 59–69.
[21] M. Lezzerini, The mortars of the «Fortezza delle Verrucole - S. Romano in Garfagnana (LU)», Per. Mineral. 74 (2005) 55-67.
[22] E. Pecchioni, F. Fratini, E. Cantisani, The ancient mortars, an attestation of the material culture: the case of Florence, Per. Mineral. 75 (2006) 255–262.
[23] A. Morricone, A. Macchia, L. Campanella, M. David, S. De Togni, M. Turci, A. Maras, C. Meucci, S. Ronca, Archaeometrical analysis for the characterization of mortars from Ostia Antica, Proc. Chem. 8 (2013) 231–238.
[24] E. Anderson, M.J. Almond, W. Matthews, Analysis of wall plasters and natural sediments from the Neolithic town of Çatalhöyük (Turkey) by a range of analytical techniques, Spectrochim. Acta A 133 (2014) 326–334.
[25] R. De Luca, M.G. Cau Ontiveros, D. Miriello, A. Pecci, E. Le Pera, A. Bloise, G.M. Crisci, Archaeometric study of mortars and plasters from the Roman City of Pollentia (Mallorca - Balearic Islands), Periodico di Mineralogia 82 (2013) 353–379.
[26] M. Lezzerini, M. Ramacciotti, F. Cantini, B. Fatighenti, F. Antonelli, E. Pecchioni, F. Fratini, E. Cantisani, M. Giamello, Archaeometric study of natural hydraulic mortars: the case of the Late Roman Villa dell'Oratorio (Florence, Italy), Archaeol. Anthropol. Sci. 9 (2017) 603–615.
[27] S. Sánchez-Moral, L. Luque, J.C. Cañaveras, V. Soler, J. Garcia-Guinea, A. Aparicio, Lime pozzolana mortars in Roman catacombs: composition, structures and restoration, Cem. Concr. Res. 35 (2005) 1555–1565.
[28] C.M. Belfiore, G.V. Fichera, M.F. La Russa, A. Pezzino, S.A. Ruffolo, G. Galli, D. Barca, A multidisciplinary approach for the archaeometric study of pozzolanic aggregate in roman mortars: the case of Villa dei Quintili (Rome, Italy), Archaeometry 57 (2015) 269–296.
[29] R. De Luca, D. Miriello, A. Pecci, S. Domínguez-Bella, D. Bernal-Casasola, A. Bloise, G.M. Crisci, Archaeometric study of mortars from the Garum Shop at Pompeii, Campania, Italy, Geoarchaeology 30 (2015) 330–351.
[30] P. Karkanas, Identification of lime plaster in prehistory using petrographic methods: a review and reconsideration of the data on the basis of experimental and case studies, Geoarchaeol: Int. J. 22 (2007) 775–796.
[31] I.A. Bany Yaseen, H. Al-Amoush, M. Al-Farajat, A. Mayyas, Petrography and mineralogy of Roman mortars from buildings of the ancient city of Jerash (Jordan), Construct. Build. Mater. 38 (2013) 465–471.
[32] M. Franzini, L. Leoni, M. Lezzerini, A procedure for determining the chemical composition of binder and aggregate in ancient mortars: its application to mortars from some medieval buildings in Pisa, J. Cult. Heritage 1 (2000) 365–373.
[33] G.M. Ingo, I. Fragalà, G. Bultrini, T. De Caro, C. Riccucci, G. Chiozzini, Thermal and microchemical investigation of Phoenician-Punic mortars used for lining cisterns at Tharros (western Sardinia, Italy), Thermochim. Acta 418 (2004) 53–60.
[34] G.M. Crisci, M. Franzini, M. Lezzerini, T. Mannoni, M.P. Riccardi, Ancient mortars and their binder, Per. Mineral. 73 (2004) 259–268.
[35] C. Genestar, C. Pons, A. Más, Analytical characterisation of ancient mortars from the archaeological Roman city of Pollentia (Balearic Islands, Spain), Anal. Chim. Acta 557 (2006) 373–379.
[36] E. Gliozzo, M.C. Dalconi, G. Cruciani, I. Turbanti, Memmi, Application of the Rietveld method for the investigation of mortars: a case study on the archaeological

site of Thamusida (Morocco), Eur. J. Mineral. 21 (2009) 457–465.

[37] G. Mertens, J. Elsen, R. Brulet, A. Brutsaert, M. Deckers, Quantitative composition of ancient mortars from the Notre Dame Cathedral in Tournai (Belgium), Mater. Character. 60 (2009) 580–585.

[38] I. Cardoso, M.F. Macedo, F. Vermeulen, C. Corsi, A. Santos Silva, L. Rosado, A. Candeias, J. Mirao, A multidisciplinary approach to the study of archaeological mortars from the town of Ammaia in the Roman Province of Lusitania (Portugal), Archaeometry 56 (2014) 1–24.

[39] D. Miriello, F. Antonelli, C. Apollaro, A. Bloise, N. Bruno, M. Catalano, S. Columbu, G.M. Crisci, R. De Luca, M. Lezzerini, S. Mancuso, A. La Marca, A petro-chemical study of ancient mortars from the archaeological site of Kyme (Turkey), Per. Miner. 84 (2015) 497–517.

[40] A. Bakolas, G. Biscontin, V. Contardi, E. Franceschi, A. Moropoulou, D. Palazzi, E. Zendri, Thermoanalytical research on traditional mortars in Venice, Thermochim. Acta 269–270 (1995) 817–828.

[41] A. Moropoulou, A. Bakolas, K. Bisbikou, Characterization of ancient, byzantine and later historic mortars by thermal and X-ray diffraction techniques, Thermochim. Acta 269–270 (1995) 779–795.

[42] S. Pagnotta, M. Lezzerini, L. Ripoll-Seguer, M. Hidalgo, E. Grifoni, S. Legnaioli, G. Lorenzetti, F. Poggialini, V. Palleschi, Micro-laser-induced breakdown spectroscopy (Micro-LIBS) study on ancient Roman mortars, Appl. Spectroscopy 71 (2017) 721–727.

[43] A. Alberti, E. Paribeni, Archeologia in Piazza dei Miracoli. Gli scavi 2003–2009,

Felici Editore Srl, Ghezzano, 2011.

[44] M. Franzini, M. Lezzerini, The stones of medieval buildings in Pisa and Lucca provinces (western Tuscany, Italy). 1 - The Monte Pisano marble, Eur. J. Mineral. 15 (2003) 217–224.

[45] M. Franzini, M. Lezzerini, Le pietre dell'edilizia medievale pisana e lucchese (Toscana occidentale). 2 I calcari selciferi del Monte Pisano, Atti Soc. Tosc. Sci. Nat. Mem. Serie A 105 (1998) 1–8.

[46] M. Lezzerini, M. Tamponi, M. Bertoli, Reproducibility, precision and trueness of X-ray fluorescence data for mineralogical and/or petrographic purposes, Atti Soc. Tosc. Sci. Nat. Mem. Serie A 120 (2013) 67–73.

[47] M. Lezzerini, M. Tamponi, M. Bertoli, Calibration of XRF data on silicate rocks using chemicals as in-house standards, Atti Soc, Tosc. Sci. Nat. Mem. Serie A 121 (2014) 65–70.

[48] G. Leone, L. Leoni, F. Sartori, Revisione di un metodo gasometrico per la determinazione di calcite e dolomite. Atti Soc. Tosc. Sci. Nat. Mem. Serie A 95 (1988) 7–20.

[49] UNI 11060 Beni culturali - Materiali lapidei naturali ed artificiali - Determinazione della massa volumica e della percentuale di vuoti. Milano: UNI - Ente Nazionale Italiano di Unificazione, 2003.

[50] M. Franzini, M. Lezzerini, A mercury-displacement method for stone bulk-density determinations, Eur. J. Mineral. 15 (2003) 225–229.

[51] H.F.W. Taylor, The Chemistry of Cements, vols. 1 and 2, London, Academic Press, 1972.